

**Mineralogy of Asteroids from Observations with the Spitzer Space Telescope.** J.P. Emery<sup>1</sup>, D.P. Cruikshank<sup>2</sup>, J. Van Cleve<sup>3</sup>, and J.A. Stansberry<sup>4</sup>. <sup>1</sup>NASA Ames/SETI Institute (Mail Stop 245-6, Moffett Field, CA, 94041; jemery@mail.arc.nasa.gov), <sup>2</sup>NASA Ames Research Center (Dale.P.Cruikshank@nasa.gov), <sup>3</sup>Ball Aerospace (jvan-cleve@ball.com), <sup>4</sup>Univ. Arizona/Steward Observatory (stansber@as.arizona.edu).

**Introduction:** Visible and near-infrared ( $\sim 0.3$  to  $4.0\ \mu\text{m}$ ) spectroscopy has been successfully employed since the early 1970's to infer the surface compositions of asteroids. Spectroscopic observations in the thermal infrared ( $\sim 5$  to  $40\ \mu\text{m}$ ) are similarly promising. Silicate spectra in this range are dominated by Si-O stretch and bend fundamentals, and other minerals have similarly diagnostic bands [e.g., 1,2]. Observations in this spectral range are difficult from the ground due to strong telluric absorptions and background emission. Nevertheless, spectral structure has been detected on a few asteroids in the 8 to  $14\text{-}\mu\text{m}$  range from the ground [3,4], as well as from orbit with the ISO satellite [e.g., 5]. The Spitzer Space Telescope can observe asteroids with much higher sensitivity over a broader wavelength range than is possible from the ground or was possible with ISO. We present results of measurements of asteroids with the Infrared Spectrograph (IRS) on the Spitzer Space Telescope.

**Overview of Observing Programs:** Several objects classified as asteroids have orbits that are dynamically similar to those of comets. These may be comets that have devolatilized by repeated passages through the inner Solar System. Reflectance spectroscopy in the vis-NIR cannot distinguish between devolatilized comets and low albedo asteroids (C-, P-, D-type asteroids); both sets of objects have low albedos and featureless spectra in the vis-NIR. In fact, the compositions of low albedo asteroids themselves are uncertain for this reason. This program undertakes a spectroscopic study of 55 asteroids in the mid-infrared ( $5.2 - 37\ \mu\text{m}$ ) in order to better understand possible links between asteroids and comets.

We also examine the spectra of Centaurs and Kuiper Belt Objects using IRS. High S/N IRS observations of the brightest sources provide compositional information, while low S/N observations of faint sources are used to constrain the albedo, size, and thermal properties of these objects. The program contains 9 Centaurs and 8 KBOs.

**Spitzer/IRS:** Spitzer is the fourth and final of NASA's Great Observatories. The sensitivity of Spitzer is 100 to 1000 times better than previous or upcoming infrared capabilities (e.g., ISO, SOFIA) over its operational spectral range of  $3.6$  to  $160\ \mu\text{m}$ . The observatory was launched into a heliocentric, Earth-trailing orbit on 25 Aug 2003 and has an expected 5 year lifetime (limited by liquid He supplies). Spitzer can track at rates fast enough for most Solar System targets, including Near Earth asteroids [6].

IRS measures spectra over the range  $5.2 - 38\ \mu\text{m}$ . The low spectral resolution mode ( $R \sim 64\text{--}128$ ) covers  $5.2 - 38\ \mu\text{m}$  in four long-slit modules. The high spectral resolution mode ( $R \sim 600$ ) covers  $10 - 37\ \mu\text{m}$  in two echelle modules (10 orders each). In addition, imaging is possible at  $16$  and  $22\ \mu\text{m}$  in the peak-up mode [7].

**A case study – 624 Hektor:** We focus our discussion here on a single asteroid as an example of the data obtained with IRS and of the analysis. Hektor is a Trojan asteroid. These asteroids orbit the sun at  $5.2\ \text{AU}$ , trapped in Jupiter's stable Lagrange points. From radiometric measurements, Hektor has an effective  $R \sim 120\ \text{km}$  and  $p_v \sim 0.04$  [8,9]. Its very large lightcurve amplitude ( $\sim 1\ \text{mag}$ ) implies a very elongated body ( $a/b \sim 2.5$ ) [10]. Recent direct imaging with HST found a similar size and elongation [11]. Vis-NIR reflectance spectroscopy reveals a red spectral slope (increasing in reflectance with wavelength) over the entire spectral range, but no absorption features [12,13,14].

**Spectral Energy Distribution (SED):** The measured SED depends on the object's size, composition, and temperature distribution. This last term is in turn dependent on several factors, including distance from the Sun, albedo, surface roughness, and thermal inertia. Spectral features in the SED are superposed on the thermal continuum, which must be removed with the use of a physical model. The simplest realistic approach is the Standard Thermal Model (STM)[15]. Our approach in this presentation uses an STM with the IAU absolute magnitude ( $H$ ) and slope ( $G$ ) parameters for the relation between albedo and size in the visible. The radius and albedo are left as free parameters, and the STM is found that best fits the measured SED. This results in an estimated  $R$  and  $p_v$ , which can be compared with previous estimates as a check on the validity of the model. For all of the objects we have observed so far, the radius and albedo from this best fit technique have agreed very well with previous measurements. Results for Hektor are shown in Fig. 1.

More complicated thermophysical models can also be applied to remove the thermal continuum [e.g., 16]. Such models require orbital and physical parameters that are not well known for many of the objects in our programs. We will use these models where appropriate. Since the thermal continua are smoothly varying functions of wavelength, "misfits" may produce an incorrect spectral slope in the final emissivity spectrum, but will not induce spurious features.

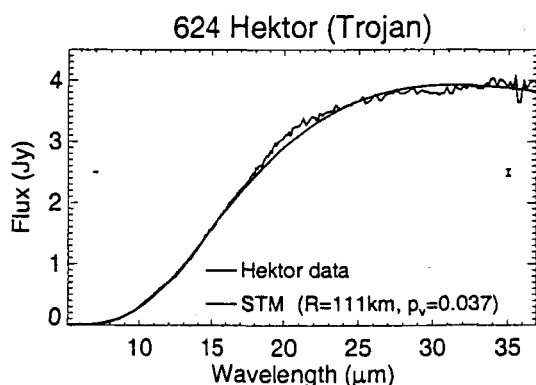


**Figure 1.** SED of 624 Hektor with corresponding best-fit thermal model. Typical error bars are shown at the short- and long-wavelength ends of the SED.

**Emissivity Spectrum:** An emissivity spectrum is created by dividing the measured SED by the modeled thermal continuum. The spectrum of Hektor is shown in Fig. 2. Compositional features are evident in this spectrum. An emission plateau from about 9 to 11.5  $\mu\text{m}$  has a spectral contrast of 10-15%, and a broad high is apparent from about 13 to 26  $\mu\text{m}$ , peaking near 20  $\mu\text{m}$ . Additionally, the spectrum rises from about 31  $\mu\text{m}$  to the end of the spectrum at 35  $\mu\text{m}$ .

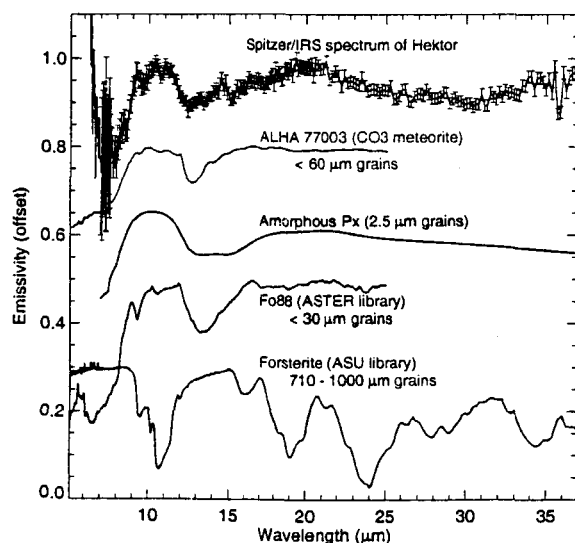


**Figure 2.** Emissivity spectrum of 624 Hektor, along with the spectrum of a carbonaceous meteorite (inverted from reflectance [1]), fine-grained pyroxene (calculated from optical constants [17]), fine-grained olivine (inverted from reflectance [1]), and coarse-grained olivine [2].

Hektor has a similar spectral shape to the carbonaceous meteorites, olivine, and pyroxene (all with small grain sizes), although the 10- $\mu\text{m}$  plateau is narrower for Hektor and its spectrum is more "peaked" near 20  $\mu\text{m}$ .

For all these spectra, the 10- $\mu\text{m}$  plateau is due to the Si-O stretch fundamental, and the 20- $\mu\text{m}$  rise is due to Si-O bend. Large grained silicates, however, have a substantially different spectral shape that does not agree well with the spectrum of Hektor. This suggests that the spectrally dominant mineral on Hektor in this wavelength range is a fine-grained silicate.

**Implications:** A silicate nature for the surfaces of Trojan asteroids has recently been suggested based on the absence of organic absorptions in the 3- to 4- $\mu\text{m}$  region and on the ability to model the vis-NIR spectra with silicates alone [13,18]. These new results from Spitzer/IRS support a silicate interpretation. This challenges the view dominant since the early 1980's that the low albedo and red spectral slopes of P- and D-type asteroids are due to organics on the surfaces [19]. The middle part of the solar nebula may not have been as rich in organic material as once thought.

**Other Asteroids and Centaurs:** We have discussed the spectrum of 624 Hektor in detail, but have also measured spectra of about 15 other asteroids, and several Centaurs. Two other Trojan asteroids (911 Agamemnon and 1172 Aneas) exhibit very similar spectral shape and contrast as Hektor. The Main Belt asteroids measured so far are more diverse. None yet have the high spectral contrast seen for Hektor, but many (particularly in the low albedo C-complex) share some of the general characteristics. We also have measured spectra of four Centaurs, one of which was bright enough to observe near 10  $\mu\text{m}$ ; the other three were only observed at  $\lambda > 15 \mu\text{m}$ . The one for which we have data near 10  $\mu\text{m}$  shows a very similar spectrum to Hektor. The other three are more diverse at the longer wavelengths. Our initial results confirm that thermal emission spectra obtained with Spitzer can be used to characterize the surface composition of asteroids.

**References:** [1] Salisbury *et al.* (1991) *Infrared (2.1-25  $\mu\text{m}$ ) Spectra of Minerals*. [2] Christensen, *et al.* (2000) *JGR*, 105(E4), 9735-9739. [3] Cohen, M. *et al.* (1998) *AJ* 115, 1671-1679. [4] Lim, L.F. *et al.* (2005) *Icarus*, in press. [5] Dotto, E., *et al.* (2002), *A&A*, 393, 1065-1072. [6] Werner, M.W., *et al.* (2004), *ApJSS*, 154, 1-9. [7] Houck, J.R., *et al.* (2004), *ApJSS*, 154, 18-24. [8] Cruikshank, D.P. (1977), *Icarus*, 30, 224-230. [9] Fernandez, Y.R., *et al.* (2003), *AJ*, 126, 1563-1574. [10] Hartmann, W.K., *et al.* (1988), *Icarus*, 73, 487-498. [11] Storrs, A.D., *et al.* (2005), *Icarus*, in press. [12] Vilas, F., *et al.* (1993), *Icarus*, 105, 67-78. [13] Cruikshank, D.P., *et al.* (2001), *Icarus*, 153, 348-360. [14] Emery, J.P. and R.H. Brown (2003), *Icarus*, 164, 104-121. [15] Lebofsky, L.A. and J.R. Spencer (1989), In *Asteroids II*, 128-136. [16] Lagerros, J.S.V. (1998), *A&A*, 332, 1123-1132. [17] Jaeger, C., *et al.* (1994), *A&A*, 292, 641-655. [18] Emery, J.P. and R.H. Brown (2004), *Icarus*, 170, 131-152. [19] Gradie, J. and J. Veverka (1980) *Nature*, 293, 840-842.